EFFECTS OF THE SPATIAL COHERENCE OF INCIDENT WAVES ON RADAR CROSS SECTION OF A CONDUCTING ELLIPTIC CYLINDER EMBEDDED IN A STRONG TURBULENT MEDIUM

Zhiqi MENG, Shingo MATSUO and Mitsuo TATEIBA
Department of Computer Science and Communication Engineering,
Faculty of Engineering, Kyushu University
6-10-1 Hakozaki, Higashi-ku, Fukuoka-shi, Fukuoka 812-81 Japan

1. Introduction

Backscattering enhancement in random media has been considered as a fundamental phenomenon which is produced by statistical coupling of incident and backscattered waves due to the effect of double passage[1–3]. If a body is surrounded with a random medium such as rain, snow, fog, and turbulence, it may then happen that the radar cross-section (RCS) of the body is remarkably different from that in free space. Therefore, the estimate of RCS of a body in a random medium has become an important subject for radar engineering and remote sensing technology. Recently a method to solve the subject as a boundary value problem has been presented; as a result, RCS of conducting circular and elliptic cylinders embedded in a strong turbulent medium have been analyzed numerically[4–6]. The numerical analysis shows that the RCS of the cylinders have been closely related to the spatial coherence of incident waves, besides the effect of double passage. Under the condition that the spatial coherence length of an incident wave is larger enough than the effective size of the cross-section of the cylinder, the RCS becomes twice as large as that in free space because of the effect of double passage. When the above condition is not satisfied, RCS changes largely; that is, it can be enhanced to more than twice as large as that in free space or diminished with the change of ka, where k is the wavenumber in free space and a is the half major axis length of the ellipse (or the radius of the circle). This result suggests that the RCS does not depend on the whole surface of the cylinder but it do on an more narrow one on which the spatial coherence of the incident wave is kept.

The numerical results of RCS were limited to $ka \leq 3$ because of the computation time. This paper deals with the analysis of RCS of a conducting elliptic cylinder in a strong turbulent medium by changing ka from zero to ten, because the larger size is expected to make further clear the effects of the spatial coherence on RCS.

Time factor $\exp(-j\omega t)$ is assumed and suppressed in the following.

2. Formulation

Consider the problem of electromagnetic wave scattering from a perfectly conducting elliptic cylinder embedded in a strong turbulent medium, as shown in figure 1. Here we deal with the backscattering of a wave which is incident on the cylinder along the z axis.

The turbulent medium is assumed to be described by the dielectric constant ε, the magnetic permeability μ and the electric conductivity σ, which are expressed as

$$\varepsilon = \varepsilon_0[1 + \delta\varepsilon(\boldsymbol{r})], \quad \mu = \mu_0, \quad \sigma = 0 \tag{1}$$

where ε_0, μ_0 are constant and $\delta\varepsilon(\boldsymbol{r})$ is a random function with

$$\langle\delta\varepsilon(\boldsymbol{r})\rangle = 0, \quad \langle\delta\varepsilon(\boldsymbol{r}) \cdot \delta\varepsilon(\boldsymbol{r}')\rangle = B(\boldsymbol{r}, \boldsymbol{r}') \tag{2}$$

Here the angular brackets $\langle\ \rangle$ denote the ensemble average and $B(\boldsymbol{r}, \boldsymbol{r})$ is the local intensity of the turbulence. For practical turbulence, the following conditions may be satisfied:

$$B(\boldsymbol{r}, \boldsymbol{r}) \ll 1, \qquad kl(\boldsymbol{r}) \gg 1 \tag{3}$$

where $k = \omega\sqrt{\varepsilon_0\mu_0}$ is the wavenumber in free space and $l(r)$ is the local scale-size of the turbulence. Because of dealing with the backscattering on the z axis as mentioned above and assuming the condition (3), it is convenient to express (2) approximately as

$$B(r, r') = B(\rho - \rho', z_+, z_-) = B(z_+)\exp\left[-\frac{z_-^2 + |\rho - \rho'|^2}{l^2(z_+)}\right] \tag{4}$$

where $r = (\rho, z)$, $r' = (\rho', z')$, $\rho = i_x x + i_y y$, $\rho' = i_x x' + i_y y'$, $z_+ = (z + z')/2$, $z_- = z - z'$, and

$$B(z_+) = \begin{cases} B_0 & , \quad a \le z \le L \\ B_0(z/L)^{-m} & , \quad L \le z \end{cases} \tag{5}$$

Here B_0 is a constant and L is a rough size of the turbulence range(see figure 1).

Let us now consider the E-wave incidence of electromagnetic waves radiated from a line source which is far from the cylinder and parallel to the y axis. Under (3), the scalar wave approximation and the forward scattering approximation are valid. Then the average intensity of backscattered waves is given by the following equation[4].

$$\begin{aligned}\langle |u_s|^2\rangle &= \int_S dr_1 \int_S dr_2 \int_S dr_1' \int_S dr_2' [Y(r_1|r_1')Y^*(r_2|r_2') \\ &\quad \langle G(r|r_1)G^*(r|r_2)G(r_1'|r_{1t})G^*(r_2'|r_{2t})\rangle]\end{aligned} \tag{6}$$

Here the asterisk denotes the complex conjugate. $G(r|r')$ is Green's function in the turbulent medium. If the turbulence is so strong that the incident wave becomes incoherent about the cylinder and we deal with only the backscattering from the cylinder, then the Green's function may be regarded as a complex Gaussian random function. In such a situation, the Fourth moment may be expressed by the product of the second moments:

$$\begin{aligned}&\langle G(r|r_1)G(r_2|r_t)G^*(r|r_1')G^*(r_2'|r_t')\rangle \\ &\simeq \langle G(r|r_1)G^*(r|r_1')\rangle\langle G(r_2|r_t)G^*(r_2'|r_t')\rangle + \langle G(r|r_1)G^*(r_2'|r_t')\rangle\langle G(r_2|r_t)G^*(r|r_1')\rangle\end{aligned} \tag{7}$$

where $r_t = r_t' = r$ on the assumptions of a single point source and backscattering. The second moments have been given in references[4, 7–9]. And Y is the current generator which can be constructed in the sense of mean by applying Yasuura's method[4, 10]:

$$\begin{aligned}Y(r|r') &= -\frac{2j}{\pi^2 c^2}\frac{1}{\sqrt{(\cosh^2\xi - \cos^2\eta)(\cosh^2\xi' - \cos^2\eta')}} \\ &\quad \left\{\sum_{n=0}^{\infty}\frac{\mathrm{ce}_n(\eta)\mathrm{ce}_n(\eta')}{\mathrm{Mc}_n^{(3)}(\xi)\mathrm{Mc}_n^{(1)}(\xi')} + \sum_{n=1}^{\infty}\frac{\mathrm{se}_n(\eta)\mathrm{se}_n(\eta')}{\mathrm{Ms}_n^{(3)}(\xi)\mathrm{Ms}_n^{(1)}(\xi')}\right\}\end{aligned} \tag{8}$$

where $ce_n(\eta)$, $se_n(\eta)$ are Mathieu's functions of the first kind. $Mc_n^{(1)}(\xi)$, $Ms_n^{(1)}(\xi)$ and $Mc_n^{(3)}(\xi)$, $Ms_n^{(3)}(\xi)$, respectively, are modified Mathieu's functions of the first and third kind. The elliptic cylindrical coordinates (ξ, η, y) used here are related to the rectangular Cartesian coordinates (z, x, y) by $z = c\cosh\xi\cos\eta$, $x = c\sinh\xi\sin\eta$, $y = y$, where c is the half focal-length of the ellipse.

3. Numerical results

From a standpoint of geometric optics, RCS will depend mainly on the illuminated surface of the ellipse. When the spatial coherence length of an incident wave is not large enough, as indicated in introduction, the RCS depends on a narrow surface S_c on which the spatial coherence of the incident wave is kept. To observe the spatial coherence of the incident wave, we define the degree of spatial coherence as

$$\Gamma(\rho, z) = \frac{\langle G(r_1|r_t)G^*(r_2|r_t)\rangle}{\langle |G(r_0|r_t)|^2\rangle} \tag{9}$$

where $r_1 = (\rho, 0)$, $r_2 = (-\rho, 0)$, $r_0 = (0, 0)$, $r_t = (0, z)$. Figure 2 shows the degrees of spatial coherence calculated from (9) in three cases: $kl_0 = 200\pi$, 20π, 2π, where $B_0kL = 3\pi$ and $z/L = 10/3$.

For the three cases of kl_0, the numerical results of RCS written as σ are shown in Figs. 3-6 with the change of ka. When the wave is incident along the minor axis of the ellipse, as shown in Figs. 3 and 4, RCS in free space (RCS_f) increases rapidly with ka. On the other hand, RCS in turbulence, for $kl_0 = 200\pi$ where the spatial coherence length of incident wave l_c is largest in the three cases, is nearly twice as large as RCS_f at first and closes to RCS_f with increasing ka, because the width of S_c is independent of ka. Increasing ka makes S_c flat, and thereby the RCS increases. For $kl_0 = 2\pi$ where l_c is the least in the three cases, the increase of RCS with ka is quite smaller than that of RCS_f, because as increasing ka, the curvature of S_c changes only a little at the center of the illuminated surface of the ellipse.

Figures 5 and 6 show RCS for the case that the wave is incident along the major axis of the ellipse. Noting that kb is a constant: 1.0 or 1.5, when ka becomes large, the curvature of the illuminated surface changes rapidly. The back-scattered wave is produced by scattering from a narrow determinative surface centered at the end point of the major axis (S_d), according to the geometrical optics approximation. As a result, RCS_f decreases with increasing ka because the increase of ka makes S_d more narrow. RCS for the turbulence of $kl_0 = 200\pi$ is nearly twice as large as RCS_f because the S_c is wider enough than S_d. For the case of $kl_0 = 2\pi$, as increasing ka, the RCS changes largely at first where S_d is wider than S_c, and is gradually close to nearly double the RCS_f because $S_d \simeq S_c$. The ellipse in Fig. 5 is more flat than that in Fig. 6, and hence the RCS in Fig. 5 comes close to nearly double the RCS_f faster than that in Fig. 6 with increasing ka.

The RCS has been analyzed in the case of wave incidence along the minor or major axis of the ellipse. In either case, the axis is coincident with the center line of wave incidence and the curvature of the illuminated surface is symmetric about the center line. When the wave is obliquely incident on the ellipse, then the curvature of the illuminated surface does not become symmetric, and as a result, RCS as a function of ka becomes more complicated especially for the case of $kl_0 = 2\pi$. The numerical results of RCS are omitted here because of the limited space.

4. Conclusion

We have analyzed numerically the radar cross sections (RCS) of a conducting elliptic cylinder in a strong turbulent medium. The numerical analysis shows that when the spatial coherence length is not larger enough than the effective size of the cross-section of the cylinder, the effects of the spatial coherence of incident waves on RCS is notable and closely related to the surface curvature.

This work was supported in part by Scientific Research Grant-In-Aid (grant 05452223, 1995) from the Ministry of Education, Science, and Culture, Japan.

References

[1] Kravtsov Yu A and A I Saichev 1982 *Sov. Phys. Usp.* 25 7 494-508
[2] Kuga Y and A Ishimaru 1984 *J. Opt. Soc. Am. A* 1 8 831-835
[3] John S 1993 *Photonic band gaps and localization* 1-22
[4] M Tateiba and Z Q Meng 1996 *PIER 14: Electromagnetic Scattering by Rough Surfaces and Random Media* (to be published in 1996)
[5] M Tateiba and Z Q Meng 1995 *Proc. 15th URSI Symp. on EMT* 637-639 (Russia)
[6] Z Q Meng and M Tateiba 1995 *Proc. APMC'95*, 1, 352-355, Taejon, Korea.
[7] Tateiba M 1985 *Radio Sci.* 20 5 1019-1024
[8] Tateiba M 1982 *Radio Sci.* 17 6 1531-1535
[9] Tateiba M 1991 *Radio Sci.* 26 2 499-503
[10] Yasuura K 1971 *Progress in Radio Science 1966-1969* 257-270 (URSI, Brussels)

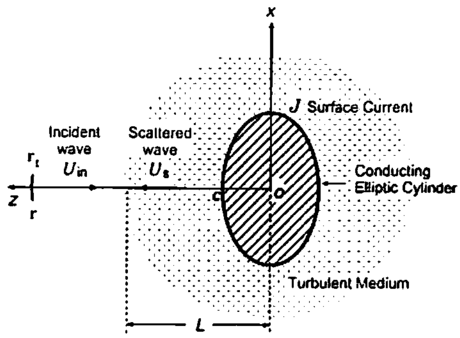

Fig. 1 Geometry of the scattering problem from a conducting elliptic cylinder

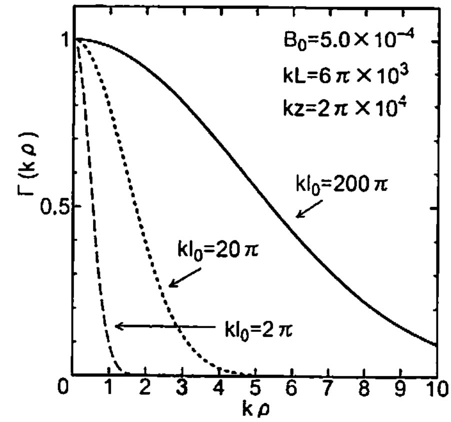

Fig. 2 The degree of spatial coherence of an incident wave about the cylinder

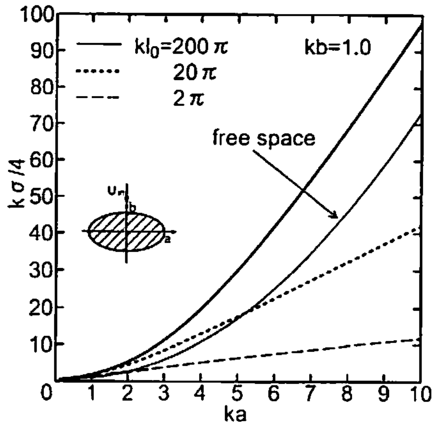

Fig. 3 RCS for wave incidence along the minor axis of the ellipse, where $kb = 1.0$ is fixed

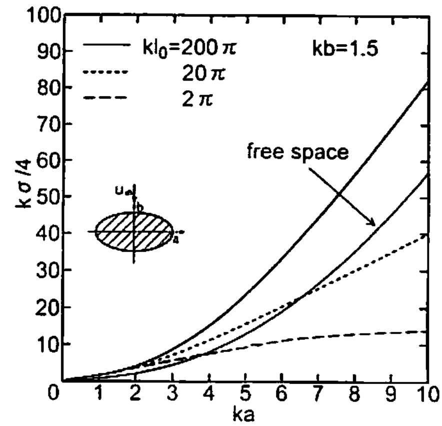

Fig. 4 RCS for wave incidence along the minor axis of the ellipse, where $kb = 1.5$ is fixed

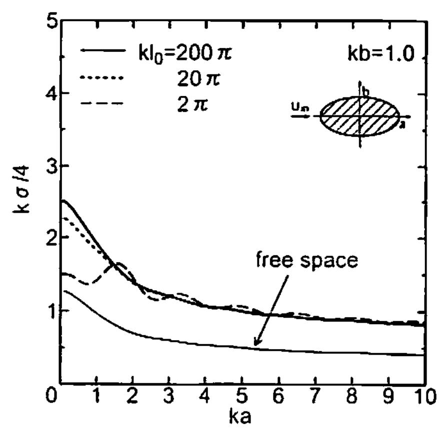

Fig. 5 RCS for wave incidence along the major axis of the ellipse, where $kb = 1.0$ is fixed

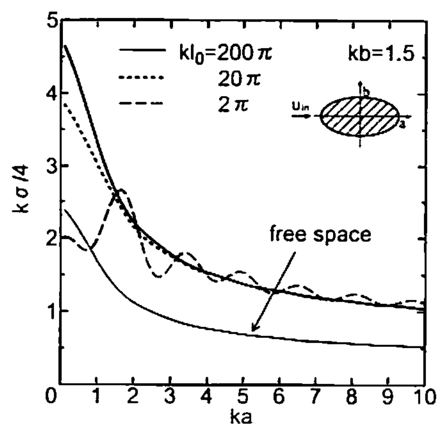

Fig. 6 RCS for wave incidence along the major axis of the ellipse, where $kb = 1.5$ is fixed